Advanced glycation end-products and *Porphyromonas gingivalis* lipopolysaccharide increase calprotectin expression in human gingival epithelial cells

Yuka Hiroshima[1*], Eijiro Sakamoto[2], Kaya Yoshida[3], Kaori Abe[4], Koji Naruishi[2], Takenori Yamamoto[1], Yasuo Shinohara[1], Jun-ichi Kido[2], Carolyn L. Geczy[5]

[1]Institute for Genome Research, Tokushima University, 3-18-15 Kuramoto, Tokushima 770-8503, Japan

[2]Department of Periodontology and Endodontology, Institute of Biomedical Sciences, Tokushima University Graduate School, 3-18-15 Kuramoto, Tokushima 770-8504, Japan

[3]Department of Oral Healthcare Education, Institute of Biomedical Sciences, Tokushima University Graduate School, 3-18-15 Kuramoto, Tokushima 770-8504, Japan

[4]SHIBASAKI, Inc., 507 Horikiri, Chichibu 368-0066, Japan

[5]School of Medical Sciences, University of New South Wales, Sydney 2052, New South Wales, Australia

**Corresponding author:* Yuka Hiroshima, DDS, PhD

Institute for Genome Research, Tokushima University

3-18-15 Kuramoto, Tokushima 770-8503, Japan

Tel: +81 88 633 9147, Fax: +81 88 634 6425

E-mail: yuka.hiroshima@tokushima-u.ac.jp

Running title: EFFECTS OF AGE AND PGLPS ON CALPROTECTIN

Keywords: **Calprotectin, Advanced glycation end-products, *Porphyromonas gingivalis* lipopolysaccharide, Human gingival epithelial cells**

Total number of text figures: 7

Total number of text tables: 0

Contract grant sponsor: JSPS KAKENHI; Contract grant number: JP15H06451 and JP17K17352

Abstract

Accumulation of advanced glycation end-products (AGEs) in periodontal tissues of patients with diabetes mellitus aggravates periodontitis, but the mechanisms are unknown. Calprotectin, a heterocomplex of S100A8 and S100A9 proteins, is a constitutive cytoplasmic component of healthy gingival epithelial cells. This study aimed at investigating the effects of AGE and *Porphyromonas gingivalis* lipopolysaccharide (PgLPS) on calprotectin expression in the human gingival epithelial cell line OBA-9. AGE and PgLPS increased the expression of S100A8 and S100A9 mRNAs, and AGE+PgLPS co-stimulation amplified their expression in OBA-9 cells. A higher concentration of calprotectin in cell lysates was also induced by stimulation with AGE and/or PgLPS. S100A8 was mainly translocated from the nucleus to the cytoplasm by AGE stimulation, while cytoplasmic localization of S100A9 was not altered following stimulation with AGE and/or PgLPS. Calprotectin was found in the cytoplasm of BSA-treated cells, but cytoplasmic and nuclear localization was observed following stimulation with AGE and/or PgLPS. AGE-induced S100A8, and S100A9 mRNA expression was partially suppressed by RAGE-specific siRNA. In contrast, PgLPS-induced S100A8 and S100A9 mRNA expression was strongly suppressed by TLR2-specific siRNA. Furthermore, the inhibition of p38, JNK MAPK, and NF-κB attenuated AGE- and PgLPS-induced S100A8 and S100A9 mRNA expression. Taken together, these results demonstrate that AGE acts in synergy with PgLPS to stimulate RAGE and TLR2 expression and activate p38, JNK MAPK, and NF-κB signaling pathways, resulting in increased activation of calprotectin (S100A8/S100A9) in

human gingival epithelial cells. Our results suggest that calprotectin may be involved in the pathogenesis of diabetic periodontitis.

Introduction

Periodontitis is a chronic oral inflammatory disease that results in loss of attachment, bone destruction, and eventually loss of teeth. Periodontitis is caused by various periodontal pathogens, such as *Porphyromonas gingivalis*, and their major outer membrane component, lipopolysaccharide (LPS) (Slots and Ting, 1999). Diabetes mellitus is a major risk factor for periodontitis. In fact, patients with diabetes mellitus exhibit greater prevalence and more extensive and severe periodontitis compared with those without diabetes mellitus (Lakschevitz et al., 2011). Both periodontitis and diabetes mellitus are chronic disorders inducing inflammation; therefore, an enhanced inflammatory response to periodontal pathogens under a diabetic condition is considered to increase the severity and the progress of periodontitis (Salvi et al., 1997). However, the molecular mechanisms by which diabetes mellitus aggravates periodontitis are not fully elucidated.

The advanced glycation end-products (AGEs) generated by chronic hyperglycemia are known to accelerate the diabetic complications, including diabetic nephropathy, diabetic ocular disease, diabetic peripheral neuropathy, and cardiovascular disorders (Goh and Cooper 2008). In periodontitis aggravated by diabetes mellitus (known as diabetic periodontitis), accumulation of AGEs is thought to be involved in the pathogenesis of chronic and intense inflammatory responses. For example, the serum levels of AGEs from patients with diabetes mellitus were associated with deterioration of periodontitis, especially attachment loss (Takeda et al., 2006). Additionally, immunoreactivity of AGEs was increased in gingival tissue from patients with diabetic periodontitis

(Zizzi et al., 2013). Furthermore, the major receptor for AGE (RAGE) is widely distributed within gingival epithelium, especially in epithelial cells and migrating leukocytes, in patients with diabetic periodontitis, whereas its expression is very weak in healthy gingiva (Abbass et al., 2012). AGE-RAGE interactions trigger various intercellular signaling cascades, including mitogen-activated protein kinases (MAPK), such as the extracellular-signal regulated kinase (Erk), p38, and c-Jun N-terminal kinase (JNK). AGE-mediated signaling via RAGE also leads to the activation of the transcription factor nuclear factor-kappaB (NF-κB), followed by induction of inflammatory mediators, such as cytokines and growth factors (Ott et al., 2014). These findings suggest that accumulation of AGEs may be involved in the worsening of diabetic periodontitis through the activation of MAPK and NF-κB pathways.

Calprotectin, a heterocomplex of S100A8 and S100A9 proteins, is a calcium-binding protein that comprises ~40% of neutrophil cytosol, being present in lower amounts in blood monocytes (Geczy et al., 2014). Calprotectin is induced in several other cell types, including epithelial cells, macrophages, and fibroblasts, by inflammatory mediators such as TLR-agonists or by oxidative stress (Hsu et al., 2009). We previously reported that calprotectin is implicated in the inflammatory activity in periodontitis. In clinical studies, calprotectin was detected in the gingival crevicular fluid (GCF, a fluid exudate that flows from the gingival margins), and its levels in GCF from patients with periodontitis were significantly higher than those in individuals without periodontitis (Kido et al., 1998, Kido et al., 1999, Nakamura et al., 2000), suggesting that calprotectin is an inflammatory

marker for diagnosis of periodontitis. In human neutrophils, the release of calprotectin was promoted by *Porphyromonas gingivalis* lipopolysaccharide (PgLPS), via a CD14-Toll-like receptor 2 (TLR2)-NF-κB pathway (Kido et al., 2003). The expression of calprotectin in epithelial cells is also regulated by factors that modulate inflammation and cell differentiation (Mork et al., 2003, Hayashi et al., 2007) and is increased by IL-1α through the p38 MAPK pathway (Bando et al., 2010). Recently, Kajiura *et al.* showed that total calprotectin amounts in GCF samples from patients with diabetic periodontitis were twice as much as those from patients with diabetes mellitus (Kajiura et al., 2014). Moreover, it was reported that AGE increased the expression of S100A8 and S100A9 mRNAs through RAGE and MAPK pathways in rat dental pulp cells (Nakajima et al., 2015). Based on these findings, we hypothesized that calprotectin induced by AGE and PgLPS may affect the pathogenesis of diabetic periodontitis. Therefore, in this study, we focused on the effects of AGE and PgLPS on S100A8 and S100A9 expression in gingival epithelial cells and investigated mechanisms underlying these AGE- and PgLPS-mediated events.

Materials and methods

Preparation of advanced glycation end-products (AGEs)

AGE-bovine serum albumin (BSA) was prepared as described elsewhere (Sakamoto et al., 2016). Briefly, 50 mg/ml BSA (Sigma-Aldrich, St. Louis, MO, USA) was incubated, under sterile conditions, with 0.1 M DL-glyceraldehyde (low endotoxin, Sigma) in 0.2 M phosphate buffer (pH 7.4), at 37°C for 7 days, and dialyzed against phosphate-buffered saline (PBS). For the control, non-glycated BSA was treated identically except that glyceraldehyde was not used. The characteristic specific fluorescence (excitation at 370 nm/emission at 440 nm) of the AGE generated was 42.5-fold greater than that of BSA controls. Endotoxin levels in all preparations were measured using kits (Wako Pure Chemical Industries, Osaka, Japan) and found to be < 5 EU/mg protein. All results are shown relative to BSA controls.

Cell culture

The Simian virus-40 (SV40) antigen-immortalized human gingival epithelial cell line OBA-9 was kindly provided by Prof. Shinya Murakami (Osaka University Graduate School of Dentistry, Osaka, Japan). OBA-9 cells were seeded at 1.5×10^4 cells/well in 12-well plastic culture plates (Sumitomo Bakelite, Tokyo, Japan) and cultured in keratinocyte-SFM (Thermo Fisher Scientific, Waltham, MA, USA) supplemented with 30 μg/ml bovine pituitary extract, 0.2 ng/ml epidermal growth factor, 100 units/ml penicillin, and 100 μg/ml streptomycin (all from Thermo Fisher Scientific), at 37°C in 5%

CO_2. Before addition of BSA, AGE, or PgLPS (from *P. gingivalis* ATCC 33277, Wako, Cat. No. 120-06351), OBA-9 cells were incubated in medium without bovine pituitary extract and epidermal growth factor, for 3 h. For RNA analysis by quantitative real-time PCR, OBA-9 cells were incubated with BSA or AGE (100-500 μg/ml), in the presence or absence of PgLPS (1 μg/ml), for 6, 12, 24, or 48 h. For protein analysis by enzyme-linked immunosorbent assay (ELISA), immunocytochemistry, and/or western blotting, OBA-9 cells were incubated with BSA or AGE (500 μg/ml), in the presence or absence of PgLPS (1 μg/ml), for 24, 36, or 48 h.

Quantitative real-time polymerase chain reaction (PCR)

Total RNA was isolated from OBA-9 cells using RNeasy Plus Micro and Mini Kit (Qiagen, Valencia, CA, USA) and cDNA synthesized from 500 ng total RNA using PrimeScript RT Master Mix (Perfect Real Time, TaKaRa Bio, Otsu, Japan). Quantitative real-time PCR was performed using StepOne Plus (Applied Biosystems, Foster City, CA, USA). Template cDNA was mixed with Fast SYBR® Green Master Mix (Thermo Fisher Scientific), distilled water, and primers. The reaction was performed at 95ºC for 20 sec, followed by 40 cycles at 95ºC for 3 sec and at 60ºC for 30 sec. The following primer sets were used: S100A8 forward, 5'-GGGATGACCTGAAGAAATTGCTA-3', and S100A8 reverse, 5'-TGTTGATATCCAACTCTTTGAACCA-3'; S100A9 forward, 5'-GTGCGAAAAGATCTGCAAAATTT-3', and S100A9 reverse,

5’-GGTCCTCCATGATGTGTTCTATGA-3’; RAGE forward, 5’-TCCAGGATGAGGGGATTTTC-3’, and RAGE reverse, 5’-CCAAGTGCCAGCTAAGAGTC-3’; TLR2 forward, 5’-GCCAAAGTCTTGATTGATTGG-3’, and TLR2 reverse, 5’- TTGAAGTTCTCCAGCTCCTG-3’; GAPDH forward, 5’-GAGTCAACGGATTTGGTCGT-3’, and GAPDH reverse, 5’-GACAAGCTTCCCGTTCTCAG-3’. The relative mRNA levels of the various genes were normalized to that of glyceraldehyde-3-phosphate dehydrogenase (GAPDH) mRNA, as an internal control.

ELISA

After 36 or 48 h stimulation with BSA or AGE (500 μg/ml), in the presence or absence of PgLPS (1 μg/ml), cells were lysed as described by (Hiroshima et al., 2016) and calprotectin in lysates measured using a sandwich ELISA kit from R&D Systems (Minneapolis, MN, USA), as per manufacturer’s instructions.

Immunocytochemistry

OBA-9 cells cultured on sterile 18-mm, round coverslips for 24 h with or without stimulants were used for immunocytochemistry. Cells were washed in PBS, fixed with 4% paraformaldehyde solution for 10 min at room temperature, and permeabilized with 0.5% Triton X-100 in PBS for 5

min. After blocking with 10% normal goat serum and 0.1% Triton X-100 in PBS for 1 h at room temperature and washing with 0.1% Triton X-100 in PBS, cells in the coverslips were first incubated overnight, at 4°C, with rabbit polyclonal anti-S100A8 (1:200 v/v; Abcam Ltd., Cambridge, MA, USA), anti-S100A9 (1:200 v/v, Abcam), mouse monoclonal anti-calprotectin [27E10] (1:50 v/v, Abcam), or normal rabbit IgG (Santa Cruz Biotecnology, Santa Cruz, CA, USA) and, then, with donkey anti-rabbit IgG H&L (DyLightr® 488, 1:200 v/v, Abcam) or goat anti-mouse IgG H&L (Alexa Fluor® 488, 1:1000 v/v, Abcam), for 1 h at room temperature, in the dark. Anti-calprotectin [27E10] antibody recognizes an epitope on the calprotectin that is not exposed on the individual subunits. Cells were then treated with DAPI solution in PBS (1:1500 v/v, Dojindo, Kumamoto, Japan) for nuclear staining. Samples were mounted and observed using an inverted fluorescence microscope (ECLIPSE Ti-U, Nikon, Tokyo, Japan).

Western blotting

Cell lysates prepared using RIPA buffer (Pierce, Rockford, IL, USA) containing 100 μM pervanadate and complete proteinase inhibitor mixture (Roche Diagnostics, Basel, Switzerland) were centrifuged at 14,000 × *g*, for 15 min, after disruption by sonication on ice. Total protein content of resulting supernatants was measured using BCA Protein Assay Kit (Thermo Fisher Scientific), standardized to BSA, according to the manufacturer's protocol. Ten micrograms of protein with 50 mM dithiothreitol was subjected to 10% SDS-PAGE, transferred to polyvinylidene

fluoride (PVDF) membranes (Merck Millipore, Darmstadt, Germany), and western blotting performed, unless otherwise stated, using the following antibodies from Cell Signaling Technology (Danvers, MA, USA): rabbit monoclonal anti-Erk1/2 (1:1000 v/v), anti-phospho-p38 MAPK (Thr^{180}/Tyr^{182}, 1:1000 v/v), anti-phospho-NF-κB p65 (Ser^{536}, 1:1000 v/v), rabbit polyclonal anti-TLR2 (1:1000 v/v), anti-phospho-Erk1/2 MAPK (Thr^{202}/Tyr^{204}, 1:1000 v/v), anti-p38 MAPK (1:1000 v/v), anti-JNK (1:1000 v/v), anti-NF-κB p65 (1:1000 v/v), anti-IκBα (1:1000 v/v), mouse monoclonal anti-phospho-JNK (Thr^{183}/Tyr^{185}, 1:1000 v/v), and anti-RAGE (1:250 v/v; R&D Systems). Anti-GAPDH antibody (1:1000 v/v, rabbit monoclonal) was used to control for protein loading. After washing with 0.1% Tween 20 in TBS, membranes were incubated with HRP-conjugated goat anti-rabbit IgG (1:10000 v/v; GE Healthcare Life Sciences, Tokyo, Japan) or sheep anti-mouse (1:5000 v/v; GE Healthcare), at room temperature for 1 h, and reactivity visualized using SuperSignal West Femto Substrate (Thermo Fisher Scientific) and Image Quant LAS-3000 UV mini imager (Fujifilm, Tokyo, Japan).

Knockdown of RAGE and TLR2 mRNAs in OBA-9 cells by small interfering RNA (siRNA)

Small interfering RNA targeting RAGE or TLR2 and a negative control siRNA (no significant homology to any known mouse, rat, or human gene sequences) were purchased from Sigma-Aldrich. OBA-9 cells seeded at 7.5×10^4 cells/well in 24-well plastic culture plates (Sumitomo Bakelite) were grown for 24 h until 80% confluence. Cells were then transfected with siRNA complexes

using Lipofectamin® RNAiMAX Reagent (Thermo Fisher Scientific), according to the manufacturer's instructions. The final concentration of siRNA transfected was 50 nM. After 24 h, total RNA and protein were extracted to confirm knockdown of RAGE and TLR2. Cells were cultured with BSA or AGE (500 μg/ml), in the presence or absence of PgLPS (1 μg/ml), for 24 and 36 h to examine expression of S100A8 and S100A9 mRNAs and to measure the concentration of calprotectin in cell lysates by ELISA, respectively. Data was analyzed using the negative control siRNA as baseline for mRNA knockdown efficiency.

Inhibition of MAPK and NF-κB signaling pathways

To investigate potential pathways contributing to AGE-induced S100A8 and S100A9 expression, OBA-9 cells were or not pre-treated for 1 h with the following inhibitors used at the given concentrations: U0126 (MEK inhibitor, 10 μM), SB203580 (p38 MAPK inhibitor, 5 μM), SP600125 (JNK inhibitor, 20 μM), and BAY11-7082 (NF-κB inhibitor, 5 μM) (all purchased from Wako). After inhibitor pre-treatment, OBA-9 cells were cultured with BSA or AGE (500 μg/ml), in the presence or absence of PgLPS (1 μg/ml), for further 24 h.

Statistical analysis

All experiments were performed at least three times to confirm the reproducibility of the results. The results are shown as the mean ± SD of three independent experiments. The mean values of the

groups were compared by one-way ANOVA in conjunction with Holm-Sidak's multiple comparisons test. Statistical significance was set at $P < 0.05$. GraphPad Prism 6.00 software (GraphPad Software, Inc., La Jolla, CA, USA) was used for data analysis.

Results

Dose effect of AGE on S100A8 and S100A9 mRNAs in OBA-9 cells

The effects of AGE on the expression of S100A8 and S100A9 mRNAs in OBA-9 cells were investigated by quantitative real-time PCR. OBA-9 cells were cultured with 100, 250, or 500 μg/ml BSA or AGE, for 24 h. As shown in Figure 1A, BSA did not change S100A8 or S100A9 mRNA levels compared with unstimulated controls. AGE significantly promoted induction of S100A8 mRNA in a dose-dependent manner (100 μg/ml: $^{*}P < 0.05$; 250 and 500 μg/ml: $^{**}P < 0.01$), whereas S100A9 mRNA was significantly induced only at 500 μg/ml AGE ($^{**}P < 0.01$). The strongest effect was detected at 500 μg/ml AGE, which increased S100A8 and S100A9 mRNA levels (2.4-fold and 1.9-fold, respectively, $^{\#\#}P < 0.01$, compared with 500 μg/ml BSA). These results suggest that, in OBA-9 cells, S100A8 mRNA may be more readily induced by AGE than S100A9 mRNA. We, thus, decided to treat OBA-9 cells with BSA or AGE at a concentration of 500 μg/ml in the subsequent experiments.

AGE and PgLPS increase S100A8 and S100A9 mRNA levels in OBA-9 cells

The time course effects of BSA or AGE (500 μg/ml), in the presence or absence of PgLPS (1 μg/ml), on S100A8 and S100A9 mRNAs in OBA-9 cells was investigated by quantitative real-time PCR (Fig. 1B). In preliminary experiments, we examined a dose range of 10-1000 ng/ml PgLPS on S100A8 and S100A9 mRNAs in OBA-9 cells, for 24 h, and determined 1 μg/ml PgLPS to be the

effective dose (data not shown). AGE caused moderate induction of S100A8 and S100A9 mRNAs within 6 h, with levels maintained up to 48 h (S100A8: 2.7-fold, $^{**}P < 0.01$; S100A9: 1.8-fold, $^{**}P < 0.01$, compared with BSA after 48 h). PgLPS also caused moderate induction of S100A8 and S100A9 mRNAs, peaking at 24 h (S100A8: 3.0-fold, $^{**}P < 0.01$; S100A9: 2.9-fold, $^{**}P < 0.01$, compared with BSA). Co-stimulation with AGE and PgLPS markedly augmented induction of S100A8 and S100A9 mRNAs after 6 h (S100A8: 5.2-fold, $^{**}P < 0.01$; S100A9: 3.6-fold, $^{**}P < 0.01$, compared with BSA), and this induction remained elevated up to 48 h (S100A8: 7.1-fold, $^{**}P < 0.01$; S100A9: 3.5-fold, $^{**}P < 0.01$, compared with BSA) (Fig. 1B). Induction of S100A8 mRNA in OBA-9 cells co-stimulated with AGE and PgLPS was consistently greater than that of S100A9 mRNA at different time points.

The concentration of calprotectin (S100A8/S100A9) in cell lysates and supernatants of OBA-9 cells was measured by ELISA 48 h after treatment with BSA or AGE in the presence or absence of PgLPS (Fig. 1C). AGE significantly increased calprotectin concentration in cell lysates ($^{**}P < 0.01$, compared with BSA). Co-stimulation with AGE and PgLPS had an additive effect on the concentration of calprotectin ($^{\#}P < 0.05$, compared with AGE). The concentration of calprotectin in the supernatants of cells treated with BSA was 18% of that in the cell lysates. AGE significantly increased calprotectin protein production, and co-stimulation with AGE and PgLPS induced further calprotectin in supernatants.

Localization of S100A8, S100A9, and calprotectin in OBA-9 cells

To examine the localization of S100A8, S100A9, and calprotectin in OBA-9 cells, and whether their locations were changed by the presence of AGE, in the presence or absence of PgLPS for 24 h, immunocytochemistry was performed (Fig. 2). Figure 2A shows that S100A8 was observed in the nuclear and perinuclear regions in BSA-treated cells. Following AGE stimulation, S100A8 fluorescence intensities appeared extremely elevated in the nuclei of some cells. PgLPS strongly induced S100A8 reactivity within particular areas of the nucleus, and fluorescence following co-stimulation with AGE and PgLPS appeared as a composite of the two stimulants. In contrast, S100A9 was observed around the nuclear membrane and in the cytoplasm in BSA-treated cells, and the pattern did not appear to change following AGE stimulation (Fig. 2B). When the cells were co-stimulated with AGE and PgLPS, S100A9 was observed mainly on the nuclear envelope and in the cytoplasm. Figure 2C shows that calprotectin was found predominantly in the cytoplasm in BSA-treated cells, but, following AGE and/or PgLPS stimulation, the expression was evident in the cytoplasm and nuclear compartments. As shown in Figure 2D, images of cells stained with normal rabbit IgG control antibody (negative control) indicated weak, non-specific reactivity that was not typical of the anti-S100A8, -S100A9, or -calprotectin antibodies.

AGE increased RAGE but not TLR2 levels

AGE and PgLPS were reported to bind to RAGE and TLR2, respectively, and induce signal

transduction (Ott et al., 2014, Kocgozlu et al., 2009). We, therefore, examined the effects of AGE and PgLPS on RAGE and TLR2 expression in OBA-9 cells. Figure 3A shows that RAGE mRNA increased by 1.5-fold following stimulation with AGE for 6 h, and the level was maintained up to 24 h ($^{*}P < 0.05$, $^{**}P < 0.01$, compared with BSA). PgLPS had an insignificant effect on RAGE mRNA level. The level of RAGE mRNA was slightly increased by co-stimulation with AGE and PgLPS for 24 h compared with AGE alone, but there was no significant difference for 6-24 h. As shown in Figure 3B, TLR2 mRNA was significantly increased by approximately 2-fold by PgLPS for 6-24 h ($^{**}P < 0.01$, compared with BSA). AGE did not affect TLR2 mRNA. Therefore, co-stimulation with AGE and PgLPS did not amplify the expression of TLR2 mRNA (compared with co-stimulation with BSA and PgLPS).

Western blotting confirmed RAGE and TLR2 protein levels in cells stimulated with BSA or AGE (500 μg/ml), in the presence or absence of PgLPS (1 μg/ml) for 24 h (Fig. 3C and D). Figure 3C shows that RAGE protein levels were significantly increased by AGE ($^{*}P < 0.05$, compared with BSA) and by co-stimulation with AGE and PgLPS ($^{**}P < 0.01$, compared with BSA). The effect of co-stimulation with AGE and PgLPS on RAGE protein levels seems to be additive. On the other hand, TLR2 protein levels were significantly increased by PgLPS ($^{**}P < 0.01$, compared with BSA; Fig. 3D) but not by AGE, neither at mRNA nor at protein levels. Therefore, TLR2 protein levels in cells co-stimulated with AGE and PgLPS were similar to those in cells co-stimulated with BSA and PgLPS (Fig. 3D). These results indicated that RAGE expression was significantly increased by

AGE and marginally by PgLPS and that TLR2 expression was enhanced only by PgLPS.

Effects of RAGE or TLR2 knockdown on S100A8 and S100A9 expression

To determine whether RAGE or TLR2 mediates the expression of S100A8 and S100A9 induced by AGE and/or PgLPS, the levels of RAGE or TLR2 in OBA-9 cells were down-regulated using specific siRNAs. First, the efficiency of siRNA knockdown in RAGE and TLR2 expression in OBA-9 cells was validated. RAGE- or TLR2-specific siRNAs-transfected cells showed similar levels of suppression of RAGE or TLR2 mRNA (right panel) and protein (left panel), by more than 70% (Fig. 4A and 4B, respectively. $^{**}P < 0.01$).

As shown in Figure 4C, stimulation with AGE or PgLPS for 24 h increased S100A8 mRNA expression, and co-stimulation with AGE and PgLPS amplified the expression (left, white bar). Down-regulation of RAGE by RAGE-specific siRNA partially suppressed S100A8 mRNA expression increased by AGE or AGE+PgLPS (black bar), whereas TLR2-specific siRNA markedly reduced its expression (gray bar). Stimulation with AGE or PgLPS also increased S100A9 mRNA expression, and co-stimulation with AGE and PgLPS showed additional induction (right, white bar). Down-regulation of RAGE by RAGE-specific siRNA significantly suppressed S100A9 mRNA expression (black bar), and TLR2-specific siRNA markedly reduced its level (gray bar).

Consistent with the results of mRNA expression, the concentration of calprotectin in cell lysates was reduced by RAGE- and by TLR2-specific siRNA following stimulation with AGE or

PgLPS. When cells were co-stimulated with AGE and PgLPS, the reduction caused by TLR2-specific siRNA on calprotectin production was more pronounced than that of RAGE-specific siRNA (Fig. 4D).

Roles of MAP kinases in S100A8 and S100A9 induction by AGE and PgLPS

Binding of AGEs to RAGE (Ott et al., 2014) and of PgLPS to TLR2 (Kocgozlu et al., 2009) activate MAPK signaling pathways. We next examined phosphorylation levels of MAPK proteins such as Erk, p38, and JNK in OBA-9 cells by western blotting. An increase in Erk, p38, and JNK phosphorylation was observed within 15 min after either AGE or PgLPS stimulation (Fig. 5A). PgLPS sustained the levels of phosphorylation for 60 min more than AGE. Moreover, we observed that co-stimulation with AGE and PgLPS activated phosphorylation of Erk, p38, and JNK within 15 min and declined thereafter. Particularly, co-stimulation with AGE and PgLPS for 15 min resulted in the greatest increase in the phosphorylation levels of Erk and p38 compared to co-stimulation with BSA and PgLPS, whereas the phosphorylation levels of JNK were not altered.

To further investigate possible signaling pathways mediating S100A8 and S100A9 induction, OBA-9 cells were pretreated with the MEK inhibitor U0126, p38 inhibitor SB203580, and JNK inhibitor SP600125, for 1 h before addition of BSA or AGE, in the presence or absence of PgLPS (Fig. 5B). The p38 and JNK inhibitors substantially reduced the induction of S100A8 and S100A9 mRNAs by AGE and/or PgLPS. The MEK inhibitor U0126 had little effect on the induction of

S100A8 or S100A9 mRNA by AGE and/or PgLPS. Similarly, pre-treatment with another MEK inhibitor, PD98095 (10 μM), had little effect on AGE- and/or PgLPS-mediated the induction of S100A8 or S100A9 mRNA (data not shown).

Involvement of NF-κB p65 in S100A8 and S100A9 induction by AGE and PgLPS

As NF-κB is activated by both AGE and PgLPS through their receptors (Ott et al., 2014, Liew et al., 2005), we examined phosphorylation levels of NF-κB in OBA-9 cells stimulated with AGE and/or PgLPS, by western blotting. Figure 6A shows that AGE and/or PgLPS increased the phosphorylation of NF-κB and that it was maintained up to 60 min after stimulation. Figure 6B shows that AGE or PgLPS induced degradation of IκBα (which binds to NF-κB) in cells stimulated for 60 min; co-stimulation with AGE and PgLPS had a more profound effect.

OBA-9 cells were pre-treated with the specific NF-κB inhibitor BAY11-7082 for 1 h before addition of BSA or AGE, in the presence or absence of PgLPS (Fig. 6C). The NF-κB inhibitor BAY11-7082 strongly attenuated AGE- and/or PgLPS-induced expression of S100A8 and S100A9 mRNAs. These results indicate that S100A8 and S100A9 mRNA inductions by AGE and/or PgLPS are likely regulated through activation of p38 and JNK MAPK and NF-κB signaling pathways, but that MEK may not be involved.

Discussion

Diabetes mellitus increases inflammation in periodontal tissues. Several studies have demonstrated that AGEs are a key factor to elucidate the pathological mechanisms underlying diabetic complications. However, little is known about the molecular mechanisms of the relationship between AGEs and periodontal tissues. Previous studies have shown that accumulation of AGEs enhanced oxidative stress and exaggerated the response to pathogens in gingival tissues (Schmidt et al., 1996). Accumulation of AGEs under the condition of periodontitis may be related to an exacerbated inflammation and may accelerate destruction of the periodontal tissues. Although recent studies have demonstrated that co-stimulation with AGE and PgLPS (a potent factor in periodontitis) increased inflammatory-related markers *in vitro* (Chiu et al., 2016, Sakamoto et al., 2016), the effects of AGE and PgLPS on gingival epithelial cells and the underlying signal mechanisms involved are not fully understood.

Calprotectin (S100A8/S100A9) is a constitutive cytoplasmic component of healthy gingival epithelial cells (Ross and Herzberg, 2001, Hiroshima et al., 2011) and is regulated as part of an epithelial cell autonomous response to infection and inflammation (Nisapakultorn et al., 2001, Mork et al., 2003, Hayashi et al., 2007). Calprotectin also has a broad range of antibacterial functions against *P. gingivalis*, other bacteria, and fungi (Champaiboon et al., 2009, Nisapakultorn et al., 2001, Zaia et al., 2009). In this study, we found that both AGE and PgLPS increased S100A8 and S100A9 mRNA expression, and co-stimulation with AGE and PgLPS amplified their expression in OBA-9

cells (Fig. 1B). In agreement with the mRNA results, concentrations of calprotectin in cell lysates were induced by AGE and/or PgLPS (Fig. 1C). Concentrations of calprotectin in supernatants were low, given that calprotectin is unlikely to be secreted by epithelium into the extracellular space under normal growth conditions. Our results demonstrated that the upregulation of calprotectin in gingival epithelial cells may primarily function intracellularly in gingival epithelial cells and may contribute to the pathological process in diabetic periodontitis.

In addition, we found that both AGE and PgLPS induced IL-6 mRNA expression, and co-stimulation with AGE and PgLPS amplified the expression in OBA-9 cells. The concentrations of IL-6 in the supernatants from OBA-9 cells were also increased by AGE and/or PgLPS. In contrast, AGE did not alter IL-8 mRNA expression, although PgLPS significantly increased the expression, which is consistent with the results of a previous study (Savitri et al., 2015). Interestingly, co-stimulation with AGE and PgLPS decreased IL-8 mRNA expression and protein levels in OBA-9 cells (Supplemental figure 1). A previous study showed that co-stimulation with high glucose and PgLPS resulted in up-regulation of IL-6 and IL-8 mRNA expression in human gingival epithelial cells. Consistent with our results, IL-8 was not altered by high glucose (Yang et al., 2014). These inflammatory cytokines secreted from gingival tissues in diabetic periodontitis may exacerbate inflammation and cause the destruction of periodontal tissues.

S100A8 and S100A9 proteins are not always co-expressed as calprotectin (Geczy et al., 2014). However, it was not clear whether S100A8 and S100A9 location and that of the complex are

changed by stimulation with AGE and/or PgLPS in gingival epithelial cells. Herein, we addressed their locations in OBA-9 cells (Fig. 2). In this study, S100A8 was mainly located in nuclear and perinuclear compartments. Stimulation with AGE and/or PgLPS increased S100A8 immunoreactivity in the nucleus (Fig. 2A). High S100A8 nuclear reactivity was also found in keratinocytes following ultraviolet A irradiation, and its expression inhibited by anti-oxidants (Grimbaldeston et al., 2003). Since S100A8 is a potent scavenger of reactive oxygen species (ROS) (Gomes et al., 2013, Lim et al., 2011), it is possible that high S100A8 nuclear reactivity may occur as a consequence of ROS generation caused by AGE accumulation in gingival epithelial cells. On the other hand, S100A9 was located around the nuclear membrane and in the cytoplasm, apparently associated with cytoskeletal structures (Fig. 2B). S100A9 reactivity was not altered by stimulation with AGE and/or PgLPS. These results may be relevant to previous reports that indicated that S100A9 is associated with tubulin filaments in activated monocytes and oral epithelial cells, promoting their release into the extracellular compartment via a tubulin-dependent pathway (Rammes et al., 1997, Zaia et al., 2009).

Calprotectin was observed in the cytoplasm and the perinuclear area in BSA-treated cells (Fig. 2C), in agreement with previous observations in human gingival keratinocytes (Ross and Herzberg, 2001). Calprotectin functions to protect epithelial cells. Intracellular calprotectin in epithelial cells increases the activation of NADPH oxidase and enhances ROS levels, which are potent microbicides against invading pathogens (Hsu et al., 2009). In addition, intracellular calprotectin is

known to function as a negative regulator of cell division and growth in keratinocytes by causing G2/M cell cycle arrest, and it is predicted to localize to the nucleus during cell division and when controlling the G2/M checkpoint (Khammanivong et al., 2013). Following stimulation with AGE and/or PgLPS, the complex was found not only in the cytoplasm but also in the nucleus, suggesting that calprotectin may suppress accelerated cell growth mediated by AGE and/or PgLPS to maintain gingival epithelial barrier functions against infection and inflammation by supporting the repair of damaged tissues, although a clear difference in cell growth was not observed in this study. Taken together, these results suggest that AGE- and/or PgLPS-induced S100A8, S100A9, and calprotectin may function independently in human gingival epithelial cells and that S100A8 and calprotectin, particularly, may contribute to avoid the exacerbation of diabetic periodontitis. Further studies on the intracellular functions of calprotectin in gingival epithelial cells are essential for determining how increased levels of calprotectin function in diabetic periodontitis.

It is well accepted that RAGE is a major receptor for AGEs and interacts with many other ligands, including amyloid β peptide, S100/calgranulin protein, high mobility group box1 (HMGB1), and LPS (Ott et al., 2014). A previous study revealed that LPS induced the upregulation of RAGE expression in alveolar type I epithelial cells (Li et al., 2014). Here, we observed that OBA-9 cells express RAGE and showed that AGE significantly increased the expression of RAGE. Additionally, co-stimulation with AGE and PgLPS induced the upregulation of RAGE expression (Fig. 3A, C). These results are consistent with *in vivo* studies using immunohistochemical staining

in human gingival tissue showing that RAGE was widely distributed and increased within gingival epithelium in patients with diabetic periodontitis (Abbass et al., 2012). Binding of AGEs to RAGE stimulates various intracellular signaling pathways, including MAPKs and NF-κB (Ott et al., 2014). Interestingly, NF-κB induced further expression of RAGE, and upregulation of RAGE activated binding sites for RAGE-ligands such as AGEs, HMGB1, and S100/calgranulin protein, perpetuating proinflammatory signals (Bierhaus et al., 2005, Li and Schmidt, 1997). Therefore, AGE stimulation may lead to an induction of RAGE expression through positive feedback of RAGE-induced NF-κB activation. However, the precise mechanism behind AGE-induced RAGE requires further analysis in gingival epithelial cells. On the other hand, the expression of TLR2 was enhanced by PgLPS but not by AGE, neither at mRNA nor at protein levels (Fig. 3B, D). Previous studies have shown that PgLPS activates both TLR2 and TLR4 (Darveau et al., 2004, Yu et al., 2016). Under our experimental conditions, however, the TLR4 gene was expressed at very low levels in OBA-9 cells, and PgLPS did not enhance the expression of TLR4 compared with TLR2 (data not shown). We therefore focused only on TLR2 as the receptor of PgLPS in this study.

Next, to determine whether RAGE or TLR2 are involved in mediating calprotectin induction in gingival epithelial cells, we used specific siRNAs to individually inhibit the expression of RAGE and TLR2. Our results showed that the inhibition of RAGE signaling with specific siRNA partially suppressed AGE-stimulated upregulation of S100A8 and S100A9 mRNA expression (Fig. 4C). These results suggest that AGE may regulate the expression of S100A8 and S100A9 through

alternative receptors in addition to RAGE. In fact, AGE has been reported to be recognized by other receptors including AGE-receptor complexes (AGE-R1/OST-48, AGE-R2/80K-H, and AGE-R3/galectin-3) and members of the scavenger receptor family (SR-A, SR-B/CD36, SR-BI, SR-E/LOX-1, and FRRL-1 and -2) (Ott et al., 2014). Under our experimental conditions, RAGE-specific siRNA induced S100A8 mRNA expression and calprotectin protein following single stimulation with BSA compared to control siRNA. It is unclear whether this induction was related to RAGE-specific siRNA. These observations require further investigation to clarify the mechanism. Moreover, the inhibition of TLR2, rather than RAGE, by specific siRNA, strongly suppressed the PgLPS-induced S100A8 and S100A9 mRNA expression and markedly reduced the expression induced by co-stimulation with AGE and PgLPS (Fig. 4C). Likewise, TLR2-specific siRNA rather than RAGE-specific siRNA decreased the concentration of calprotectin induced by PgLPS (Fig. 4D). Thus, it is likely that AGE-induced S100A8 and S100A9 expression is partially dependent on RAGE, whereas PgLPS induces the expression mainly through the TLR2 pathway.

To further determine the possible mechanisms underlying the induction of S100A8 and S100A9 by AGE and PgLPS, we explored intracellular signaling pathways. Previous studies have demonstrated that both AGE and PgLPS activate multiple cascades, including MAPK (Erk, p38, and JNK) and NF-κB pathways (Liew et al., 2005, Ott et al., 2014). In agreement with previous reports, we observed increased Erk, p38, and JNK phosphorylation in OBA-9 cells within 15 min after either AGE or PgLPS stimulation, indicating that both AGE and PgLPS activate MAPK

signaling pathways (Fig. 5A). Moreover, we observed that co-stimulation with AGE and PgLPS activated phosphorylation of Erk, p38, and JNK within 15 min, declining thereafter. Furthermore, we found that pre-treatment with the p38 MAPK inhibitor SB203580 and the JNK inhibitor SP600125 strongly reduced S100A8 and S100A9 mRNA induction by AGE and/or PgLPS (Fig. 5B). In contrast, under our experimental conditions, pre-treatment with the MEK inhibitor U0126 had little effect on the induction of S100A8 or S100A9 mRNA by AGE and/or PgLPS. These results suggest that p38 and JNK participate in the upregulation of S100A8 and S100A9 expression in OBA-9 cells.

NF-κB is activated by both AGE and PgLPS through their receptors. In consonance with previous reports, we observed that stimulation with AGE and/or PgLPS increased the phosphorylation of NF-κB for 60 min after treatment (Fig. 6A). Moreover, the stimulation promoted degradation of IκBα, an important negative regulator of NF-κB signaling, and the NF-κB inhibitor BAY11-7082 attenuated the increase of S100A8 and S100A9 mRNAs induced by AGE and/or PgLPS (Fig. 6B, C).

In conclusion, this study demonstrated that AGE acts in synergy with PgLPS to stimulate RAGE and TLR2 expression and activate p38, JNK MAPK, and NF-κB signaling pathways, resulting in increased activation of calprotectin (S100A8/S100A9) in human gingival epithelial cells (Fig. 7). Although further studies are required to clearly identify functions of AGE- and/or PgLPS-induced calprotectin in gingival epithelial cells, we suggest that calprotectin may be

involved in the pathogenesis of diabetic periodontitis.

Acknowledgement

We thank Professor Shinya Murakami (Osaka University Graduate School of Dentistry) for kindly providing OBA-9 cells. This study was supported by the Support Center for Advanced Medical Sciences, Institute of Biomedical Sciences, Tokushima University Graduate School, by the Clinical Research Center for Diabetes, Tokushima University Hospital, and by JSPS KAKENHI Grant Number JP15H06451 (Grant-in-Aid for Research Activity Start-up, YH) and JP17K17352 (Grant-in-Aid for Young Scientist B, YH).

Conflict of interests

The authors declare that there is no conflict of interests regarding the publication of this paper.

References

Abbass MM, Korany NS, Salama AH, Dmytryk JJ, Safiejko-Mroczka B. 2012. The relationship between receptor for advanced glycation end products expression and the severity of periodontal disease in the gingiva of diabetic and non diabetic periodontitis patients. Arch Oral Biol 57:1342-1354.

Bando M, Hiroshima Y, Kataoka M, Herzberg MC, Ross KF, Shinohara Y, Yamamoto T, Nagata T, Kido J. 2010. Modulation of calprotectin in human keratinocytes by keratinocyte growth factor and interleukin-1α. Immunol Cell Biol 88:328-333.

Bierhaus A, Humpert PM, Morcos M, Wendt T, Chavakis T, Arnold B, Stern DM, Nawroth PP. 2005. Understanding RAGE, the receptor for advanced glycation end products. J Mol Med 83:876-886.

Champaiboon C, Sappington KJ, Guenther BD, Ross KF, Herzberg MC. 2009. Calprotectin S100A9 calcium-binding loops I and II are essential for keratinocyte resistance to bacterial invasion. J Biol Chem 284:7078-7090.

Chiu HC, Fu MM, Yang TS, Fu E, Chiang CY, Tu HP, Chin YT, Lin FG, Shih KC. 2016. Effect of

high glucose, *Porphyromonas gingivalis* lipopolysaccharide and advanced glycation end-products on production of interleukin-6/-8 by gingival fibroblasts. J Periodontal Res 52:268-276.

Darveau RP, Pham TT, Lemley K, Reife RA, Bainbridge BW, Coats SR, Howald WN, Way SS, Hajjar AM. 2004. *Porphyromonas gingivalis* lipopolysaccharide contains multiple lipid A species that functionally interact with both toll-like receptors 2 and 4. Infec Immun 72:5041-5051.

Geczy CL, Chung YM, Hiroshima Y. 2014. Calgranulins may contribute vascular protection in atherogenesis. Circ J 78:271-280.

Gomes LH, Raftery MJ, Yan WX, Goyette JD, Thomas PS, Geczy CL. 2013. S100A8 and S100A9-oxidant scavengers in inflammation. Free Radic Biol Med 58:170-186.

Grimbaldeston MA, Geczy CL, Tedla N, Finlay-Jones JJ, Hart PH. 2003. S100A8 induction in keratinocytes by ultraviolet A irradiation is dependent on reactive oxygen intermediates. J Invest Dermatol 121:1168-1174.

Hayashi N, Kido J, Kido R, Wada C, Kataoka M, Shinohara Y, Nagata T. 2007. Regulation of calprotectin expression by interleukin-1α and transforming growth factor-β in human gingival

keratinocytes. J Periodontal Res 42:1-7.

Hiroshima Y, Bando M, Inagaki Y, Kido R, Kataoka M, Nagata T, Kido J. 2016. Effect of Hangeshashinto on calprotectin expression in human oral epithelial cells. Odontology 104:152-162.

Hiroshima Y, Bando M, Kataoka M, Inagaki Y, Herzberg MC, Ross KF, Hosoi K, Nagata T, Kido J. 2011. Regulation of antimicrobial peptide expression in human gingival keratinocytes by interleukin-1α. Arch Oral Biol 56:761-767.

Hsu K, Champaiboon C, Guenther BD, Sorenson BS, Khammanivong A, Ross KF, Geczy CL, Herzberg MC. 2009. Anti-infective protective properties of S100 calgranulins. Antiinflamm Antiallergy Agents Med Chem 8:290-305.

Kajiura Y, Bando M, Inagaki Y, Nagata T, Kido J. 2014. Glycated albumin and calprotectin levels in gingival crevicular fluid from patients with periodontitis and type 2 diabetes. J Periodontol 85:1667-1675.

Khammanivong A, Wang C, Sorenson BS, Ross KF, Herzberg MC. 2013. S100A8/A9 (calprotectin) negatively regulates G2/M cell cycle progression and growth of squamous cell carcinoma. PloS one

8:e69395.

Kido J, Kido R, Suryono, Kataoka M, Fagerhol MK, Nagata T. 2003. Calprotectin release from human neutrophils is induced by *Porphyromonas gingivalis* lipopolysaccharide via the CD-14-Toll-like receptor-nuclear factor κB pathway. J Periodontal Res 38:557-563.

Kido J, Nakamura T, Kido R, Ohishi K, Yamauchi N, Kataoka M, Nagata T. 1998. Calprotectin, a leukocyte protein related to inflammation, in gingival crevicular fluid. J Periodontal Res 33:434-437.

Kido J, Nakamura T, Kido R, Ohishi K, Yamauchi N, Kataoka M, Nagata T. 1999. Calprotectin in gingival crevicular fluid correlates with clinical and biochemical markers of periodontal disease. J Clin Periodontol 26:653-657.

Kocgozlu L, Elkaim R, Tenenbaum H, Werner S. 2009. Variable cell responses to *P. gingivalis* lipopolysaccharide. J Dent Res 88:741-745.

Lakschevitz F, Aboodi G, Tenenbaum H, Glogauer M. 2011. Diabetes and periodontal diseases: interplay and links. Curr Diabetes Rev 7:433-439.

Li J, Schmidt AM. 1997. Characterization and functional analysis of the promoter of RAGE, the receptor for advanced glycation end products. J Biol Chem 272:16498-16506.

Li Y, Wu R, Zhao S, Cheng H, Ji P, Yu M, Tian Z. 2014. RAGE/NF-κB pathway mediates lipopolysaccharide-induced inflammation in alveolar type I epithelial cells isolated from neonate rats. Inflammation 37:1623-1629.

Liew FY, Xu D, Brint EK, O'Neill LA. 2005. Negative regulation of toll-like receptor-mediated immune responses. Nat Rev Immunol 5:446-458.

Lim SY, Raftery MJ, Geczy CL. 2011. Oxidative modifications of DAMPs suppress inflammation: the case for S100A8 and S100A9. Antioxid Redox Signal 15:2235-2248.

Mørk G, Schjerven H, Mangschau L, Søyland E, Brandtzaeg P. 2003. Proinflammatory cytokines upregulate expression of calprotectin (L1 protein, MRP-8/MRP-14) in cultured human keratinocytes. Br J Dermatol 149:484-491.

Nakajima Y, Inagaki Y, Kido J, Nagata T. 2015. Advanced glycation end products increase

expression of S100A8 and A9 via RAGE-MAPK in rat dental pulp cells. Oral Dis 21:328-334.

Nakamura T, Kido J, Kido R, Ohishi K, Yamauchi N, Kataoka M, Nagata T. 2000. The association of calprotectin level in gingival crevicular fluid with gingival index and the activities of collagenase and aspartate aminotransferase in adult periodontitis patients. J Periodontol 71:361-367.

Nisapakultorn K, Ross KF, Herzberg MC. 2001. Calprotectin expression in vitro by oral epithelial cells confers resistance to infection by *Porphyromonas gingivalis*. Infect Immun 69:4242-4247.

Ott C, Jacobs K, Haucke E, Navarrete Santos A, Grune T, Simm A. 2014. Role of advanced glycation end products in cellular signaling. Redox Biol 2:411-429.

Rammes A, Roth J, Goebeler M, Klempt M, Hartmann M, Sorg C. 1997. Myeloid-related protein (MRP) 8 and MRP14, calcium-binding proteins of the S100 family, are secreted by activated monocytes via a novel, tubulin-dependent pathway. J Biol Chem 272:9496-9502.

Ross KF, Herzberg MC. 2001. Calprotectin expression by gingival epithelial cells. Infect Immun 69:3248-3254.

Sakamoto E, Mihara C, Ikuta T, Inagaki Y, Kido J, Nagata T. 2016. Inhibitory effects of advanced glycation end-products and *Porphyromonas gingivalis* lipopolysaccharide on the expression of osteoblastic markers of rat bone marrow cells in culture. J Periodont Res 51:313-320.

Salvi GE, Collins JG, Yalda B, Arnold RR, Lang NP, Offenbacher S. 1997. Monocytic TNFα secretion patterns in IDDM patients with periodontal diseases. J Clin Periodontol 24: 8-16.

Savitri IJ, Ouhara K, Fujita T, Kajiya M, Miyagawa T, Kittaka M, Yamakawa M, Shiba H, Kurihara H. 2015. Irsogladine maleate inhibits Porphyromonas gingivalis-mediated expression of toll-like receptor 2 and interleukin-8 in human gingival epithelial cells. J Periodont Res 50:486-493.

Schmidt AM, Weidman E, Lalla E, Yan SD, Hori O, Cao R, Brett JG, Lamster IB. 1996. Advanced glycation endproducts (AGEs) induce oxidant stress in the gingiva: a potential mechanism underlying accelerated periodontal disease associated with diabetes. J Periodont Res 31:508-515.

Slots J, Ting M. 1999. *Actinobacillus actinomycetemcomitans* and *Porphyromonas gingivalis* in human periodontal disease: occurrence and treatment. Periodontol 2000 20:82-121.

Takeda M, Ojima M, Yoshioka H, Inaba H, Kogo M, Shizukuishi S, Nomura M, Amano A. 2006.

Relationship of serum advanced glycation end products with deterioration of periodontitis in type 2 diabetes patients. J Periodontol 77:15-20.

Yang X, Zhang J, Ni J, Ouyang B, Wang D, Luo S, Xie B, Xuan D. 2014. Toll-like receptor 4-mediated hyper-responsiveness of gingival epithelial cells to lipopolysaccharide in high-glucose environments. J Periodontol 85:1620-1628.

Yu X, Wang Y, Lin J, Hu Y, Kawai T, Taubman MA, Han X. 2016. Lipopolysaccharides-Induced Suppression of Innate-Like B Cell Apoptosis Is Enhanced by CpG Oligodeoxynucleotide and Requires Toll-Like Receptors 2 and 4. PLoS One 11:e0165862.

Zaia AA, Sappington KJ, Nisapakultorn K, Chazin WJ, Dietrich EA, Ross KF, Herzberg MC. 2009. Subversion of antimicrobial calprotectin (S100A8/S100A9 complex) in the cytoplasm of TR146 epithelial cells after invasion by *Listeria monocytogenes*. Mucosal Immunol 2:43-53.

Zizzi A, Tirabassi G, Aspriello SD, Piemontese M, Rubini C, Lucarini G. 2013. Gingival advanced glycation end-products in diabetes mellitus-associated chronic periodontitis: an immunohistochemical study. J Periodontal Res 48:293-301.

Figure legends

Figure 1. Effects of AGE and/or PgLPS on the expression of S100A8 and S100A9 mRNAs and on the production of calprotectin protein in OBA-9 cells. (A) OBA-9 cells were cultured with 100, 250, or 500 μg/ml BSA (open column) or AGE (closed column), for 24 h. S100A8 and S100A9 mRNAs were analyzed by quantitative real-time PCR. Gray columns show unstimulated controls. Data are mean ± SD of three independent experiments. *$P < 0.05$, **$P < 0.01$, compared with unstimulated control. $^{\#\#}P < 0.01$, compared with BSA. (B, C) OBA-9 cells were cultured with 500 μg/ml BSA or AGE, in the presence or absence of 1 μg/ml PgLPS, for 6, 12, 24, and 48 h (B) and for 48 h (C). (B) S100A8 and S100A9 mRNAs were analyzed by quantitative real-time PCR. (C) Concentrations of calprotectin in cell lysates and supernatants were determined by ELISA. Data are mean ± SD of three independent experiments. *$P < 0.05$, **$P < 0.01$, compared with BSA. $^{\#}P < 0.05$, $^{\#\#}P < 0.01$, compared with AGE+PgLPS.

Figure 2. Localization of S100A8, S100A9, and calprotectin in OBA-9 cells after stimulation with AGE and/or PgLPS. OBA-9 cells were cultured with 500 μg/ml BSA or AGE, in the presence or absence of 1 μg/ml PgLPS, for 24 h. Localization of S100A8 (A), S100A9 (B), and calprotectin (C) was performed by immunocytochemistry using anti-S100A8, anti-S100A9, and anti-calprotectin (green). DAPI was used to stain the nuclei (blue). (D) As negative control, cells stained with normal rabbit IgG instead of anti-S100A8, anti-S100A9, or anti-calprotectin are shown. Microscopy images

of the same field were taken and merged. Magnification, x1000; Scale bars, 5 μm. A representative image of three independent experiments is shown.

Figure 3. Effects of AGE and/or PgLPS on RAGE and TLR2 mRNA and protein expression in OBA-9 cells. OBA-9 cells were cultured with 500 μg/ml BSA or AGE, in the presence or absence of 1 μg/ml PgLPS, for 6, 12, 24, and 48 h (A, B) and for 24 h (C, D). RAGE (A) and TLR2 (B) mRNAs were analyzed by quantitative real-time PCR. Relative levels of RAGE (C) and TLR2 (D) to GAPDH in cell lysates were determined by western blotting, after SDS-PAGE separation of 10 μg protein/lane. A representative blot of three is shown. Quantitative signal intensities were measured by densitometry and are indicated below the corresponding bars. GAPDH was used as loading control. The densitometry ratio of RAGE or TLR2 normalized to that of GAPDH using NIH image is shown. Data are mean ± SD of three independent experiments. $^{*}P < 0.05$, $^{**}P < 0.01$, compared with BSA. $^{\#}P < 0.05$, $^{\#\#}P < 0.01$, compared with AGE+PgLPS.

Figure 4. The effect of RAGE and TLR2 knockdown on the expression of S100A8 and S100A9 mRNAs and on calprotectin protein levels in OBA-9 cells. OBA-9 cells were transfected with RAGE siRNA or TLR2 siRNA for 24 h (A, B) and cultured with 500 μg/ml BSA or AGE, in the presence or absence of 1 μg/ml PgLPS, for further 24 h (C) and 36 h (D). (A, B) Protein levels of RAGE (A, left) and TLR2 (B, left) were determined by western blotting. A representative blot is

shown. RAGE (A, right) and TLR2 (B, right) mRNAs were analyzed by quantitative real-time PCR. Protein and mRNA levels of RAGE and TLR2 were both reduced by 70% in cells transfected with siRNA directed to RAGE or to TLR2, compared with the negative control siRNA. (C) S100A8 and S100A9 mRNAs were analyzed by quantitative real-time PCR. (D) Calprotectin concentrations in cell lysates were determined by ELISA. Data are mean ± SD of three independent experiments. *$P < 0.05$, **$P < 0.01$, compared with control siRNA in each group.

Figure 5. Pathways contributing to induction of S100A8 and S100A9 mRNAs by AGE and PgLPS in OBA-9 cells. (A) OBA-9 cells were cultured with 500 μg/ml BSA or AGE, in the presence or absence of 1 μg/ml PgLPS, for 15, 30, and 60 min. Phosphorylated MAPKs (Erk, p38, and JNK) were assessed by western blotting. A representative blot is shown. Band density was quantified by densitometric scanning of bands for 15 min, using National Institutes of Health ImageJ software. (B) OBA-9 cells were pre-treated with U0126 (10 μM), SB203580 (5 μM), or SP600125 (20 μM) for 1 h before addition of 500 μg/ml BSA or AGE, in the presence or absence of 1 μg/ml PgLPS, for 24 h. S100A8 and S100A9 mRNAs were analyzed by quantitative real-time PCR. Data are mean ± SD of three independent experiments. *$P < 0.05$, **$P < 0.01$, compared with cells pre-treated with DMSO in each group.

Figure 6. Involvement of NF-κB in induction of S100A8 and S100A9 mRNAs by AGE and PgLPS

in OBA-9 cells. (A) OBA-9 cells were cultured with 500 μg/ml BSA or AGE, in the presence or absence of 1 μg/ml PgLPS, for 15, 30, and 60 min. Phosphorylated NF-κB was determined by western blotting. (B) OBA-9 cells were cultured with 500 μg/ml BSA or AGE, in the presence or absence of 1 μg/ml PgLPS, for 60 min. IκBα was determined by western blotting. Representative blots are shown. (C) OBA-9 cells were pre-treated with BAY11-7082 (5 μM) for 1 h before addition of 500 μg/ml BSA or AGE, in the presence or absence of 1 μg/ml PgLPS, for 24 h. S100A8 and S100A9 mRNAs were analyzed by quantitative real-time PCR. Data are mean ± SD of three independent experiments. $*P < 0.05$, compared with cells pre-treated with DMSO in each group.

Figure 7. A schematic diagram showing proposed pathway in AGE- and PgLPS-induced calprotectin (S100A8/S100A9) expression in human gingival epithelial cells. AGE/RAGE and PgLPS/TLR2 signaling activated both the MAPK (p38 and JNK) and NF-κB pathways, leading to increased calprotectin expression in human gingival epithelial cells.

Figure 1

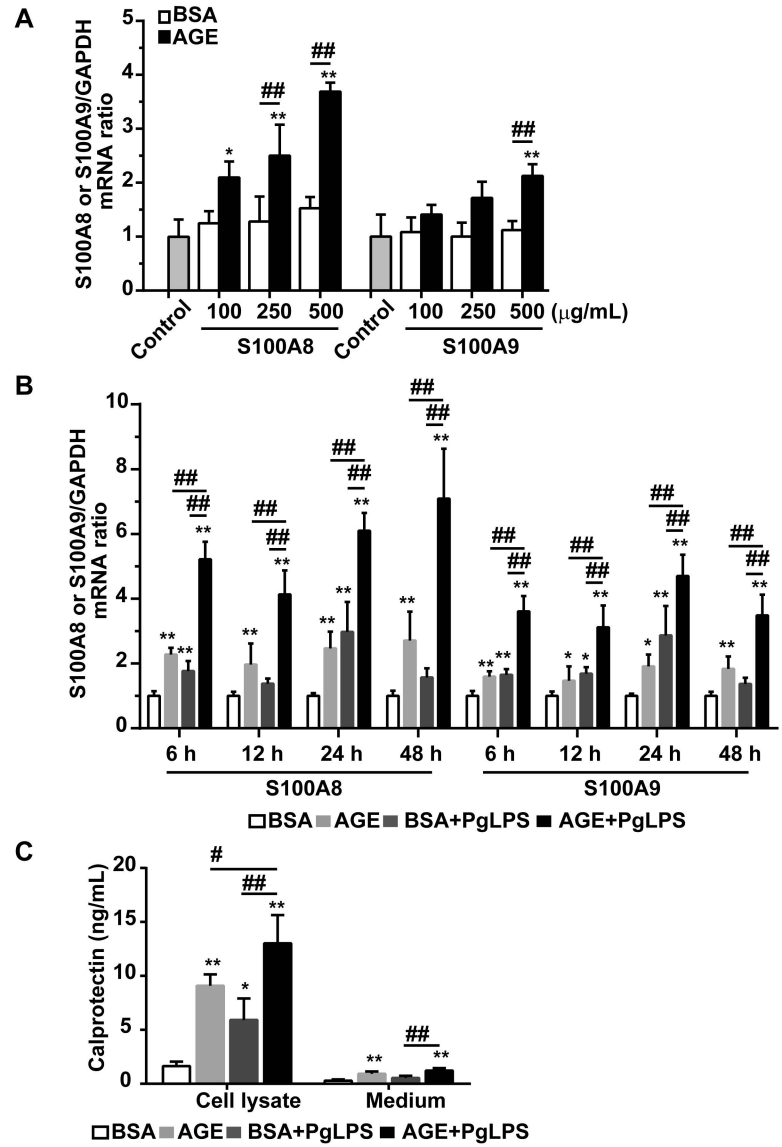
A
BSA
AGE
S100A8 or S100A9/GAPDH mRNA ratio
Control
100
250
500
S100A8
Control
100
250
500
(μg/mL)
S100A9
B
S100A8 or S100A9/GAPDH mRNA ratio
6 h
12 h
24 h
48 h
S100A8
S100A9
BSA
AGE
BSA+PgLPS
AGE+PgLPS
C
Calprotectin (ng/mL)
Cell lysate
Medium
BSA
AGE
BSA+PgLPS
AGE+PgLPS

Figure 2

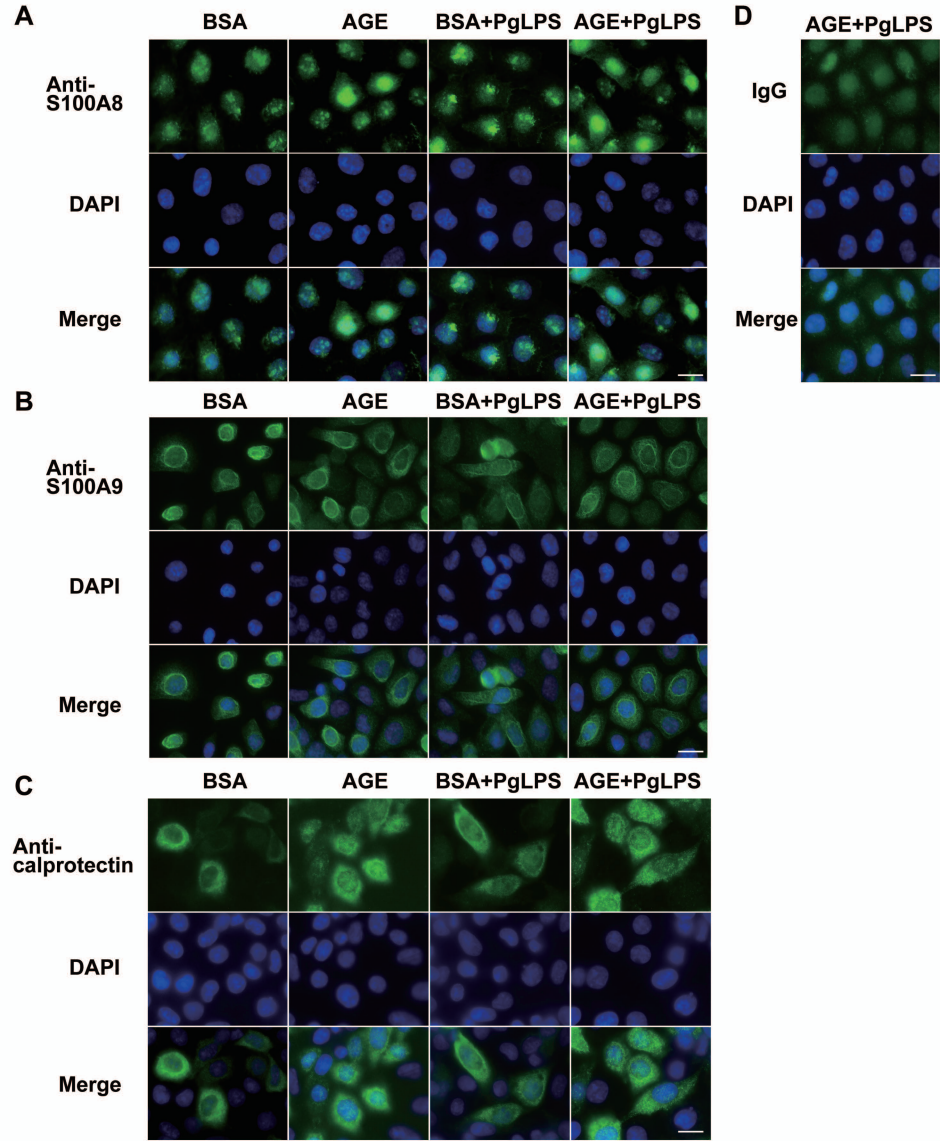
A
BSA
AGE
BSA+PgLPS
AGE+PgLPS
Anti-S100A8
DAPI
Merge
D
AGE+PgLPS
IgG
DAPI
Merge
B
BSA
AGE
BSA+PgLPS
AGE+PgLPS
Anti-S100A9
DAPI
Merge
C
BSA
AGE
BSA+PgLPS
AGE+PgLPS
Anti-calprotectin
DAPI
Merge

Figure 3

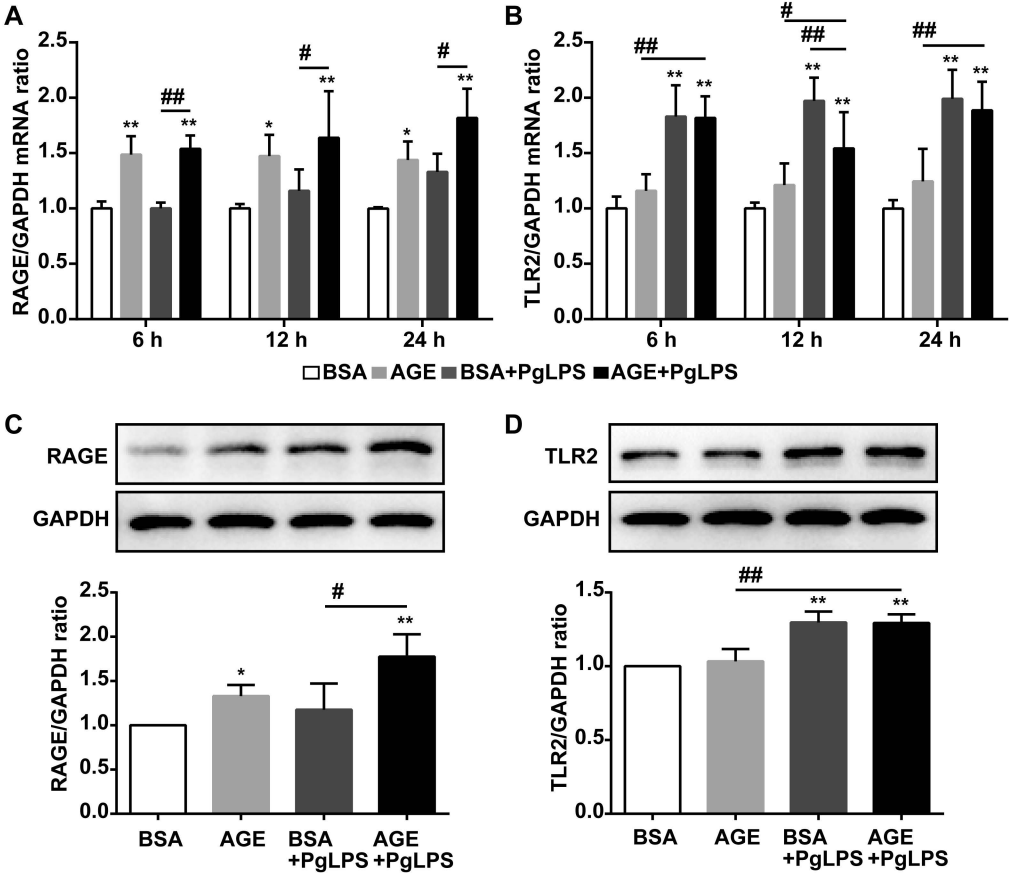
A
RAGE/GAPDH mRNA ratio
2.5
2.0
1.5
1.0
0.5
0.0
6 h
12 h
24 h
B
TLR2/GAPDH mRNA ratio
BSA
AGE
BSA+PgLPS
AGE+PgLPS
C
RAGE
GAPDH
RAGE/GAPDH ratio
BSA
AGE
BSA +PgLPS
AGE +PgLPS
D
TLR2
GAPDH
TLR2/GAPDH ratio

Figure 4

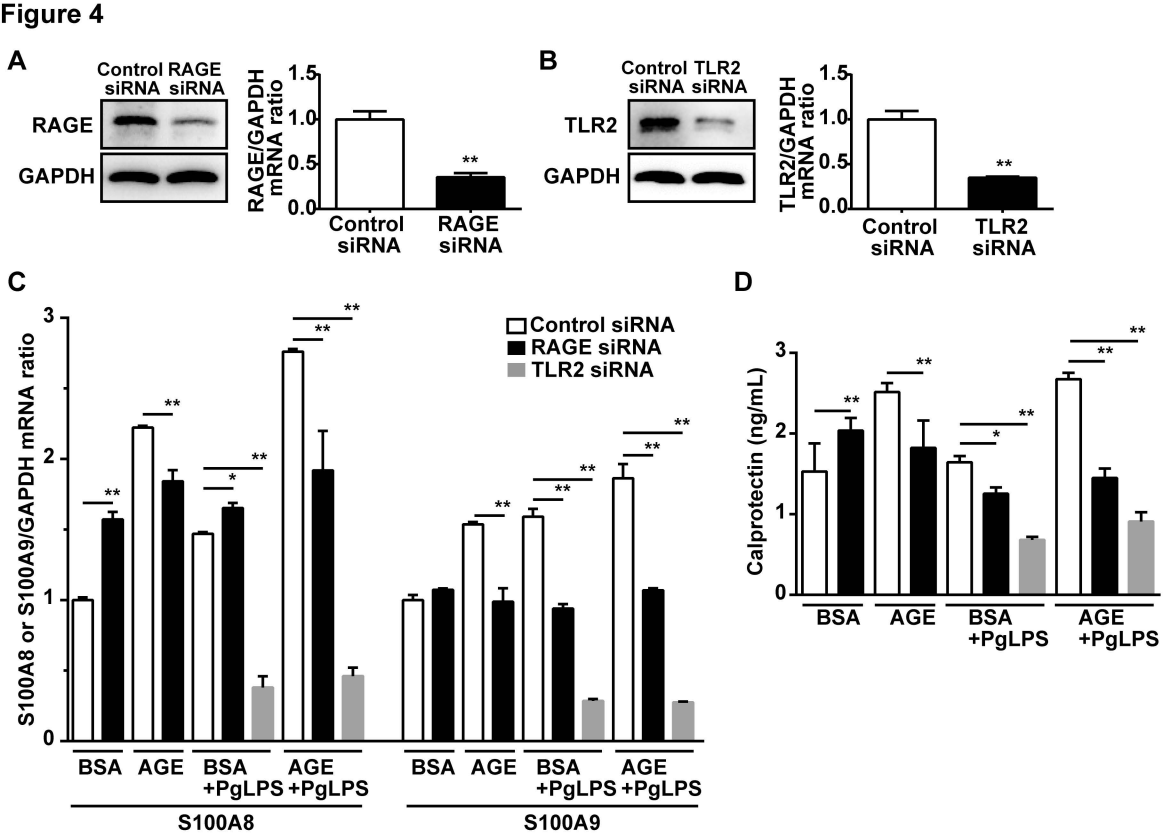
A
Control siRNA
RAGE siRNA
RAGE
GAPDH
RAGE/GAPDH mRNA ratio
1.5
1.0
0.5
0.0
**
Control siRNA
RAGE siRNA
B
Control siRNA
TLR2 siRNA
TLR2
GAPDH
TLR2/GAPDH mRNA ratio
1.5
1.0
0.5
0.0
**
Control siRNA
TLR2 siRNA
C
S100A8 or S100A9/GAPDH mRNA ratio
3
2
1
0
Control siRNA
RAGE siRNA
TLR2 siRNA
**
*
BSA
AGE
BSA +PgLPS
AGE +PgLPS
S100A8
S100A9
D
Calprotectin (ng/mL)
3
2
1
0
**
*
BSA
AGE
BSA +PgLPS
AGE +PgLPS

Figure 5

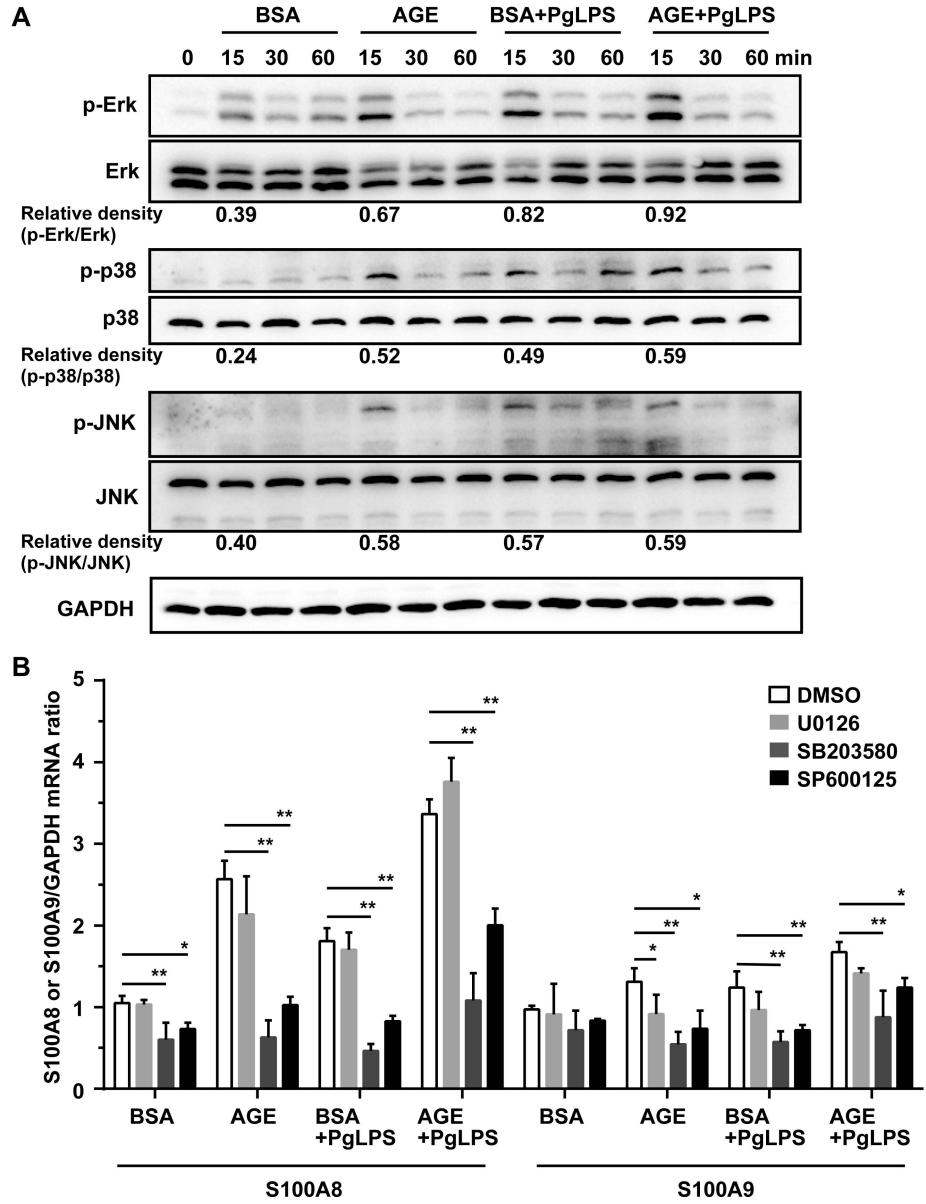
A
BSA
AGE
BSA+PgLPS
AGE+PgLPS
0 15 30 60 15 30 60 15 30 60 15 30 60 min
p-Erk
Erk
Relative density (p-Erk/Erk)
0.39
0.67
0.82
0.92
p-p38
p38
Relative density (p-p38/p38)
0.24
0.52
0.49
0.59
p-JNK
JNK
Relative density (p-JNK/JNK)
0.40
0.58
0.57
0.59
GAPDH
B
S100A8 or S100A9/GAPDH mRNA ratio
DMSO
U0126
SB203580
SP600125
BSA
AGE
BSA +PgLPS
AGE +PgLPS
S100A8
S100A9

Figure 6

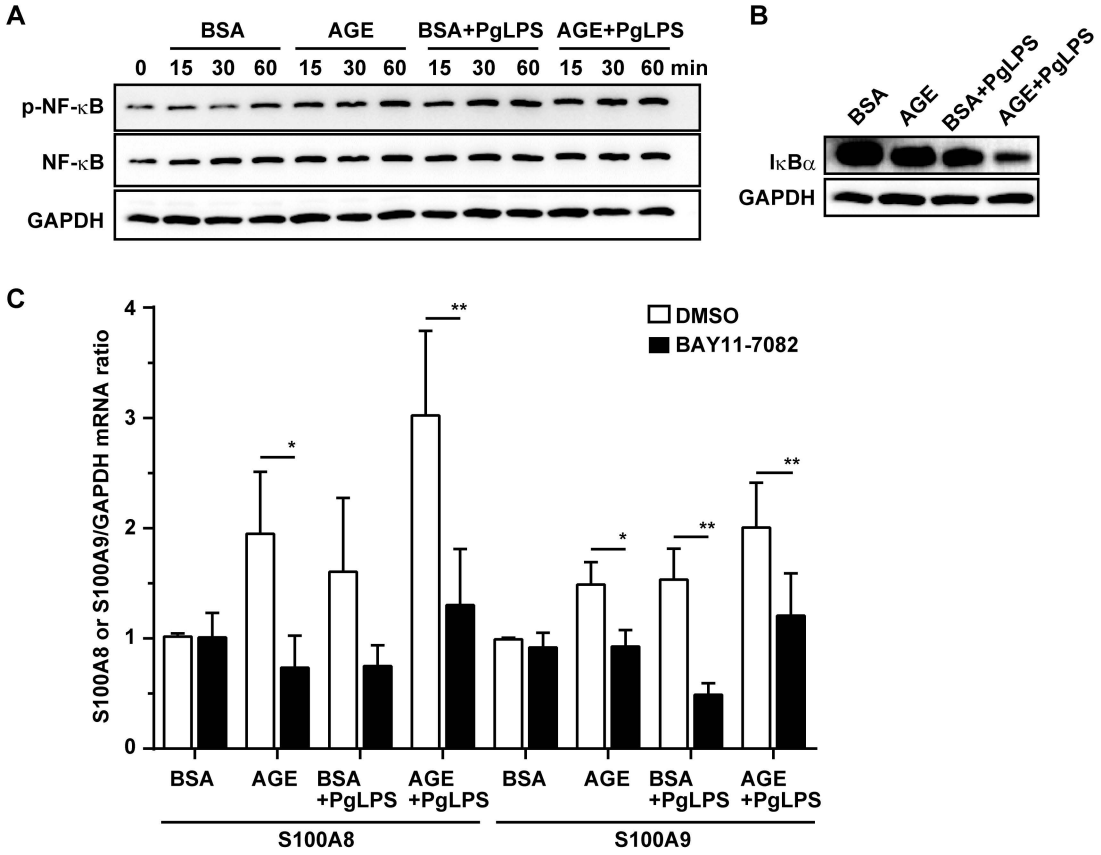
A
BSA
AGE
BSA+PgLPS
AGE+PgLPS
0 15 30 60 15 30 60 15 30 60 15 30 60 min
p-NF-κB
NF-κB
GAPDH
B
BSA
AGE
BSA+PgLPS
AGE+PgLPS
IκBα
GAPDH
C
DMSO
BAY11-7082
S100A8 or S100A9/GAPDH mRNA ratio
0
1
2
3
4
*
**
*
**
**
BSA
AGE
BSA +PgLPS
AGE +PgLPS
BSA
AGE
BSA +PgLPS
AGE +PgLPS
S100A8
S100A9

Figure 7

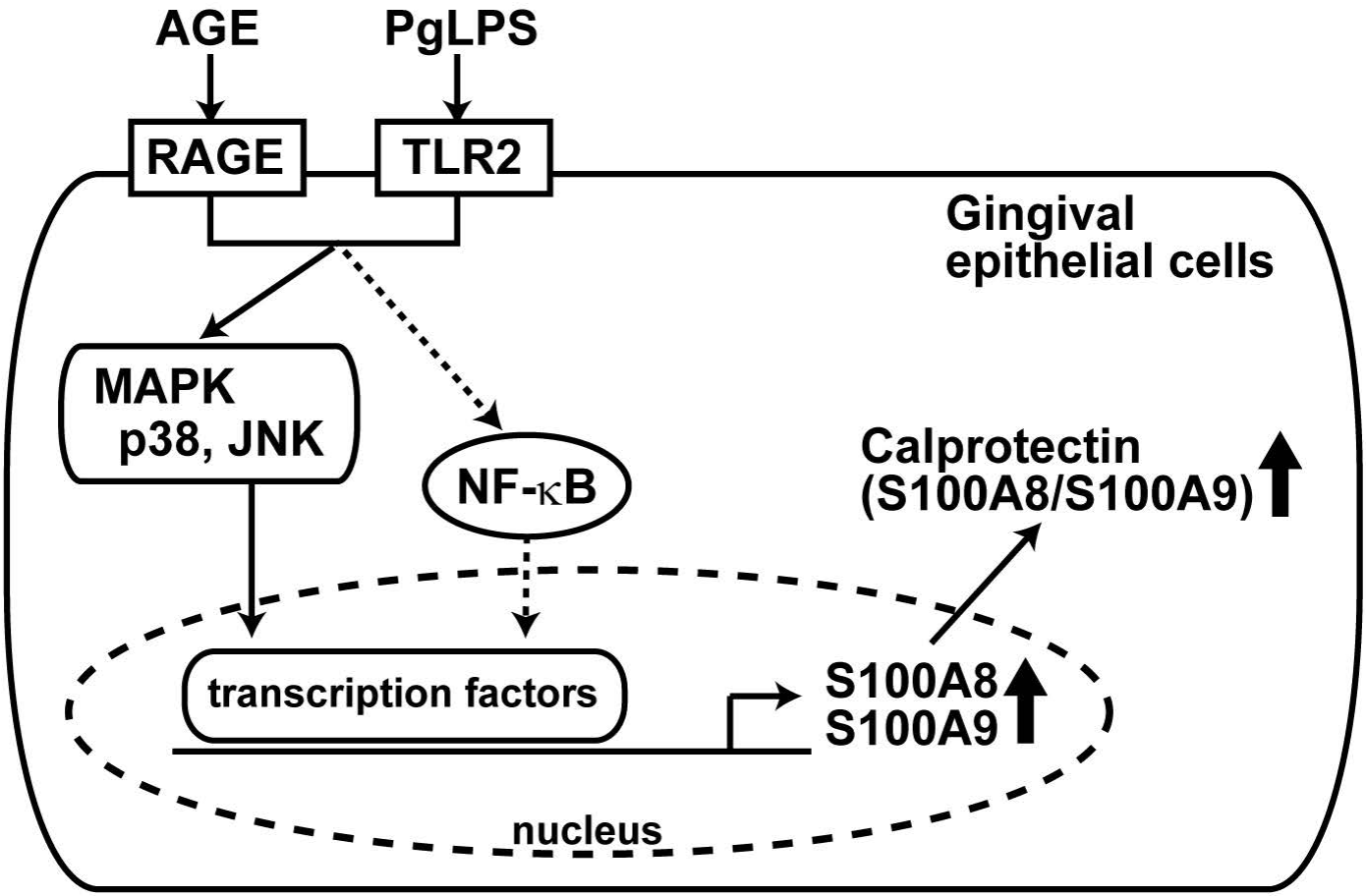
AGE
PgLPS
RAGE
TLR2
Gingival epithelial cells
MAPK p38, JNK
NF-κB
Calprotectin (S100A8/S100A9)
transcription factors
S100A8
S100A9
nucleus

Supplemental Figure 1

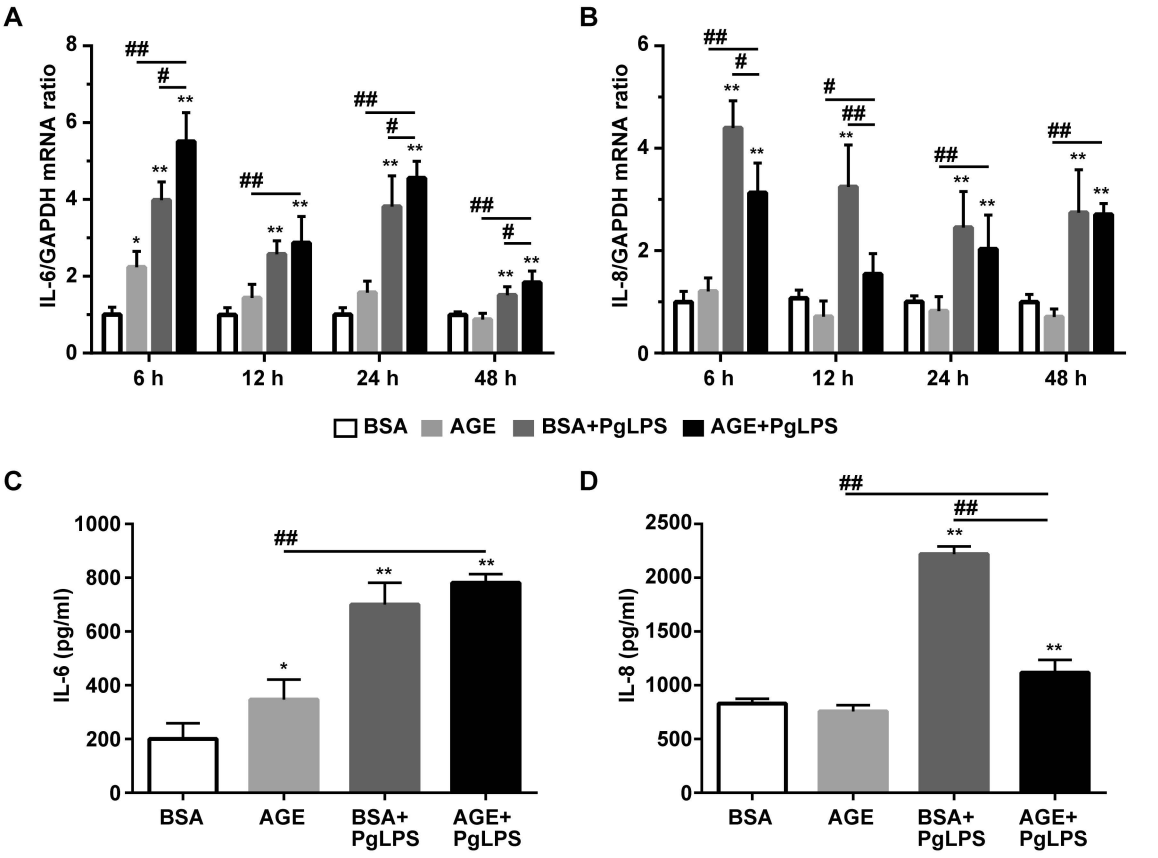

Supplemental Figure 1. Effects of AGE and/or PgLPS on IL-6 and IL-8 mRNA and protein expression in OBA-9 cells. OBA-9 cells were cultured with 500 μg/ml BSA or AGE, in the presence or absence of 1 μg/ml PgLPS, for 6, 12, 24, and 48 h. IL-6 (A) and IL-8 (B) mRNAs were analyzed by quantitative real-time PCR. OBA-9 culture supernates were collected after 24 h stimulation. Concentrations of IL-6 (C) and IL-8 (D) in supernates were determined by ELISA. Data are mean ± SD of three independent experiments. *$P < 0.05$, **$P < 0.01$, compared with BSA. #$P < 0.05$, ##$P < 0.01$, compared with AGE+PgLPS.